cDIP: Channel-aware Dynamic Window Protocol for Energy-efficient IoT Communications

Priyadarshi Mukherjee and Swades De

***Abstract*—Energy efficiency plays a critical role in widespread deployability of IoT applications. While there have been some prior studies on channel-adaptive communication strategies, these approaches do not fully exploit the channel knowledge on increasing energy efficiency in link-layer communications. In this paper we consider point-to-point IoT communication over wireless channel. We propose a generalized channel-aware link-layer communication strategy that exploits temporal variations of the communication channel to improve on energy efficiency. Specifically, we propose a generalized channel dependent communication strategy that just depends on rate of variation of the channel and not on its underlying fading distribution. We utilize this generalized information on channel state variation in dynamically deciding on the transmission and waiting windows in link-layer transmission, which gives significant benefits in terms of system throughput as well as energy efficiency by optimally using the good channel states and avoiding redundant transmission of acknowledgements. Our analytical claims and numerical results are verified through extensive simulations. Our numerical results further demonstrate that, the proposed dynamic window protocol offers a significant gain of about 40% in terms of data throughput and about 41% in terms of energy efficiency in comparison to its nearest competitive existing benchmark scheme.**

***Index Terms*—Channel-aware link-layer communication, temporal correlation, dynamic window protocol, energy-efficiency**

I. Introduction and Background

In recent years there has been a significant growth of interest on Internet of Things (IoT) and wireless sensor network (WSN) applications. According to Ericsson [1], global Internet traffic is expected to increase by nine times by the year 2022, and the IoT devices are projected to increase at a compound annual rate of 21% during this period. To support this escalating Internet traffic, energy consumption of the wireless devices is also expected to increase sharply. However, since large energy demand is unaffordable in many wireless deployment scenarios, high energy consumption of the wireless nodes is expected to be a major factor in widespread adoption of IoT and WSN deployment feasibility. As a result, relevance of energy-efficient and green communications has increased significantly [2], [3].

Limited energy resource of the field nodes in IoT and WSN applications necessitates that the energy be used prudently. In context of delay-tolerant transmission applications over licensed wireless channel as well as cognitive radio channels, various link-layer and medium access protocols have been proposed that account for the dynamic wireless channel conditions. However, yet the role of time-varying wireless channel has not been sufficiently exploited. Intuitively, proper utilization of the channel knowledge can help in judiciously deciding the transmission timing as well as the duration of channel utilization, thereby improving on both data throughput as well as energy efficiency.

In this work, we focus on the point-to-point communication from a battery-constrained wireless node to a receiver over a pre-assigned channel. We relook at the data transmission strategy and investigate the optimum usage of temporal variation of the channel condition for improved link-layer performance. We propose to modify the conventional ARQ protocol for short-range wireless communications, wherein waiting and transmission windows are dynamically decided for data transmission, which also does not require acknowledgement for all data frames thereby improving channel utilization as well as energy saving at the nodes. Since the proposed strategy does not require feedback for every data frame, it is of high relevance in low-power applications, such as battery-limited IoT communications, WSNs, and wireless-powered communication networks [4].

A. Prior Art and Motivation

In order to deal with the channel errors arising due to multipath fading, there broadly exists two categories of link-layer error control schemes, namely, automatic repeat request (ARQ) and forward error correction (FEC). In communication scenarios in dynamic channel conditions, where delay requirements are not strict, ARQ appears to be a better option compared to FEC. Conventional ARQ schemes are further classified into Stop-and-Wait (SW), Go-Back-N (GBN), and Selective-Repeat (SR). It is important to note that all of these basic link-layer ARQ strategies operate oblivious of the wireless channel conditions.

Lu and Chang [5] investigated these basic ARQ protocols in the context of correlated channel errors. Li and Zhou [6] characterized the transmission mechanism of SR protocol in terms of a discrete-time Geom/G/1/∞ queue model. Cloud *et al.* [7] proposed a coded generalization of SR protocol in order to improve application layer performance. Chakraborty *et al.* [8] looked into adaptive GBN protocol by using Gilbert-Elloit model of the wireless channel. Ausavapattanakun and Nosratinia [9] studied the throughput of GBN protocol in block fading scenarios. Pimentel and Siqueira [10] presented the analysis of GBN protocol in the context of finite state Markov Rician fading channels.

This work was supported by the Department of Science and Technology under Grant SB/S3/EECE/0248/2014.

P. Mukherjee and S. De are with the Department of Electrical Engineering and Bharti School of Telecom, IIT Delhi, New Delhi, India (e-mail: {priyadarshi.mukherjee, swadesd}@ee.iitd.ac.in).

SW protocol finds its application in various short-range communication scenarios, such as, telemetry and IoT networks, which require protocol simplicity and high energy efficiency. Benelli and Garzelli [11] proposed a few modifications in the classical SW protocol for the purpose of achieving higher throughput. De Vuyst and Bruneel [12] investigated SW protocol with temporally correlated errors. Li and Zhao [13] looked into the resequencing buffer behaviour of SW protocol in a multichannel communication scenario. However in all these link-layer data transmission strategies, energy is wasted in futile attempts of data transmission even when the channel is in deep fade.

Adaptive modulation and coding (AMC) [14]–[16] has been a fairly well-investigated topic in the context of achieving high link-layer throughput even in presence of fading. In AMC, there exists a provision (mode 0) of not sending any data payload when the channel is in deep fade. But energy is still wasted in mode 0 under severe channel condition, because feedback from the receiver is required in each time slot to decide the mode of data transmission.

On the other hand, there has been some research in the direction of channel-aware link-layer retransmissions [17]–[22]. Guth and Ha [17] proposed a feedback-dependent policy, in which the transmitted frame size is based on the number of consecutive successes and retransmissions. Minn *et al.* [18] proposed to count the successive number of ACKs (acknowledgements) or NAKs (negative ACKs) for determining the channel status to let the system configure its transmissions accordingly. Zorzi and Rao [19] proposed a probing-based retransmission approach in GBN and SR, where the transmitter sends probing signals at regular intervals upon a NAK reception until it receives a probing ACK. As it can be seen, the channel parameters did not have any impact on the probing interval duration. De *et al.* [20] proposed various channel adaptive variants of the SW protocol that aim at reducing the chances of blind retransmissions when the channel is unsuitable for data transfer. Moon [21] suggested the concept of predetermined channel sensing intervals, where data transmission takes place only if the channel state is found above a certain threshold, or else the channel is sensed again after the channel coherence time interval. Beyond the studies in [17]–[21], a recent work by Mukherjee *et al.* [22] evaluated the optimum waiting interval in link-layer retransmission based on the current channel state and long-term channel statistics, which showed improved throughput and energy efficiency.

In context of dynamic spectrum access Agarwal and De showed, for energy-optimized point-to-point communications, as in battery-constrained IoT and WSN applications, having a pre-assigned channel works better than letting the transmitter switch around multiple channels [23], [24]. Further, in single-channel access scenario they investigated optimum waiting and transmission durations for improved secondary user performance within a guaranteed limit of primary interference.

Motivated by the observation in [23], we consider that the miniature IoT/WSN transmitter node is equipped with pre-assigned wireless channels, which a node intend to maximally use while minimizing the energy consumption. Our work is aimed at complementing the prior studies in [17]–[22]. We note that, while the basic objective of exploiting the wireless channel dynamics has been appreciated by several researchers, there is a significant scope of improving the transmission performance by dynamically deciding on the optimum transmission and waiting windows as well as by avoiding unnecessary acknowledgement (ACK) transmissions. Specifically we argue that, beyond the studies in [19]–[22], by considering dynamically optimizing the transmission window along with the waiting window and by controlled ACK transmission, an overall higher transmission performance is expected. Our analysis in this work is significantly different from that in [24], which considered optimized channel utilization in presence of primary users, and also the focus was not fading channel characterization and its exploitation.

B. Contributions

Observing the lacuna discussed above, we investigate the usage of temporal variation of the wireless channel and propose a dynamic transmission and waiting window based protocol, which we call cDIP. The specific contributions and features of this work are highlighted below:

- A channel-dependent analytical framework is proposed for calculating the probability of signal strength staying above a given threshold for a given time interval.
- We formulate an optimization problem for calculating the time duration over which the channel will continue to remain above a threshold, given that it is currently above the threshold. Consequently, a minimal complexity algorithm is proposed to solve the optimization problem.
- With the optimum interval estimate, a channel-aware dynamic window size based link-layer protocol is proposed. Our results demonstrate that the data throughput and energy efficiency of the proposed protocol is respectively about 40.18% and 41.29% higher in comparison to its nearest approach.
- However, the performance gain in cDIP is at the cost of some extra overhead in terms of extra bits in the selective ACK/NAK (negative ACK) packets for conveying the current channel state information. Specifically, our results show that, about 6 bits in an ACK/NAK packet is required in the proposed cDIP as opposed to binary ACK in the conventional channel-oblivious link-layer ARQ protocols. Also, as in the SR protocol, receiver has to maintain a re-sequencing buffer [25] in order to tackle the frame re-ordering issue, so that the correctly received data frames can be orderly delivered to the higher layer.

To the best of our knowledge, cDIP is a novel approach that intelligently adjusts the data transmission timings, which has not been explored earlier. It is important to note that, *the transmission/waiting window size depends on the temporal variation of the channel, but at the same time it does not require the knowledge of the underlying fading distribution.* Dynamic estimation of transmission window also entails that, unlike the conventional SW ARQ protocol (as in [19]–[22]) it does not require ACK for every data packet. Also, quality of estimation of transmission and waiting windows imply that the probing packets during the waiting phase (as in [19],

[21]) are not necessary. By virtue of *channel-aware dynamic transmission and waiting windows* in cDIP, the proposed approach is different from the conventional SR protocol.

C. Significance

Results presented in the paper demonstrate the importance of cDIP in energy-constrained scenarios where longevity of field nodes is very critical. This work, providing insight on role of channel in determining the transmission as well as waiting interval, can also be extended to heterogeneous communication systems, where various applications require different channel conditions for operation.

The channel-aware protocol cDIP proposed in this paper is useful in a variety of emerging IoT applications where continuous stream of (possibly accumulated) data transmission over larger batches are practiced. Some examples are, smart meter data transmission to a nearby aggregator [26] data communication from a Phasor Monitoring Unit to a nearby access point or base station in smart grid networks [27]–[30], mobile infotainment and other vehicular communications [31], [32], mobile sink based field data aggregation for pollution mapping and other smart city and surveillance applications [33], [34], and mobile multimedia streaming content upload from smart gadgets in social networks [35], [36]. These IoT and smart mobile applications being mostly semi-real-time or sometimes delay-tolerant, intelligent decision on CTI and CWI for content transmission/ upload are expected to offer meaningful communication and device energy resource saving.

D. Paper Organization

The remaining paper is organized as follows. System model and the proposed protocol are described in Section II. In Section III first the concept of temporal derivative of the signal is introduced, which is followed by the determination of the optimum transmission interval for continuous data transmission. Section IV discusses the proposed protocol performance and accordingly an optimization problem is formulated that aims at maximizing the energy efficiency of the system. Section V discusses the numerical results, followed by concluding remarks in Section VI.

II. System Model and Protocol Description

A. System Model

We consider link-layer communication between a IoT wireless node pair in mobile environment, where data frames are always available at the transmitter (Tx) for transmission [19].

The system is assumed slotted, with slot duration T_s sec. It is considered that the channel remains invariant within a frame duration T_f but may vary from frame to frame [14], [15]. The consideration of a slotted communication scenario is also motivated by the fact that the practical implementations of datalink layer protocols are slot-based.

Depending on received signal quality, the receiver (Rx) sends ACK or NAK. A NAK is sent if the signal strength indicator (SSI) at Rx is below a predetermined threshold X_{TH}. Thus, the ACK/NAK decision of the Rx depends on fading envelope X of the underlying wireless channel. The channel is considered to be in 'good' state when the current channel state $X(t) = X_0$ is greater than X_{TH}, and 'bad' otherwise.

In the ACK/NAK packet, Rx also sends useful channel information, such as channel state estimate and Doppler frequency f_D. f_D estimation from received signal is known from [37], where Tepedelenlioglu *et al.* comprehensively summarized all the existing f_D estimation schemes present in literature.

f_D corresponding to relative velocity v of Rx is $f_D \cong \frac{v f_c}{c}$, where f_c is the carrier frequency and c is the velocity of light in vacuum. The product $f_D T_s$ signifies the rate of temporal variation of the channel. From [38] we know that large value of $f_D T_s$ (> 0.2) indicates an almost independent 'fast' fading channel, whereas a small value of $f_D T_s$ (< 0.1) implies a correlated 'slow' fading channel.

It should be noted that due to the presence of scatterers [39], received signal at Rx can experience Doppler effect even with stationary Tx and Rx . The factor v (or f_D) effectively captures the effect of mobility of Tx, Rx, or scatterers, or a combination of them.

B. Protocol Description

We now describe our proposed *channel-aware Dynamic wIndow Protocol (cDIP)*, based on the feedback information from Rx. The usefulness of this protocol lies in the fact that it adapts depending on the characteristics of the wireless channel. Proposed cDIP operation is explained in Fig. 1.

When the channel is in 'good' state, Tx estimates transmission window $\boldsymbol{T_{gb}}$ over which the channel will continue to be in 'good' state. Tx communicates this information to Rx and continuously transmits data frames without requiring any acknowledgement from Rx during this period. At the end of $\boldsymbol{T_{gb}}$, Rx sends a feedback packet containing SSI (X_0) information and also the information of erroneously received data frames. If $X_0 \geq X_{TH}$, Tx estimates $\boldsymbol{T_{gb}}$ and first retransmits the erroneously received data frames, followed by new data frames, and the cycle repeats.

But if $X_0 < X_{TH}$, Tx estimates waiting time $\boldsymbol{T_{bg}}$ over which the channel will continue to be in the 'bad' state. After $\boldsymbol{T_{bg}}$, Tx transmits a probing signal, and if it receives a probing ACK (alternatively, NAK), then it estimates $\boldsymbol{T_{gb}}$ (alternatively, $\boldsymbol{T_{bg}}$) accordingly, and the cycle continues. But if Tx receives garbled or no feedback from Rx (which may happen when either or both of the forward and reverse channel are in deep fade), it randomly chooses a $\boldsymbol{T_{bg}}$ with the knowledge of the latest $\boldsymbol{T_{bg}}$ as follows:

$$\boldsymbol{T_{bg}} = \mathbb{U}_{\mathbb{R}}(0,1) \times \boldsymbol{T_{bg}^{l}} \tag{1}$$

where $\mathbb{U}_{\mathbb{R}}(0,1)$ is a random number chosen from a uniform distribution in the interval $(0,1)$ and $\boldsymbol{T_{bg}^{l}}$ is the $\boldsymbol{T_{bg}}$ estimated in the recent past. After this $\boldsymbol{T_{bg}}$ period, Tx again sends a probing signal and takes decision accordingly.

It may be noted that ACK/NAK feedback consumes energy. Hence cDIP aims at reducing the frequency of these feedback packets using the channel knowledge, which is eventually reflected in terms of higher energy efficiency of cDIP in comparison to its nearest competitor.

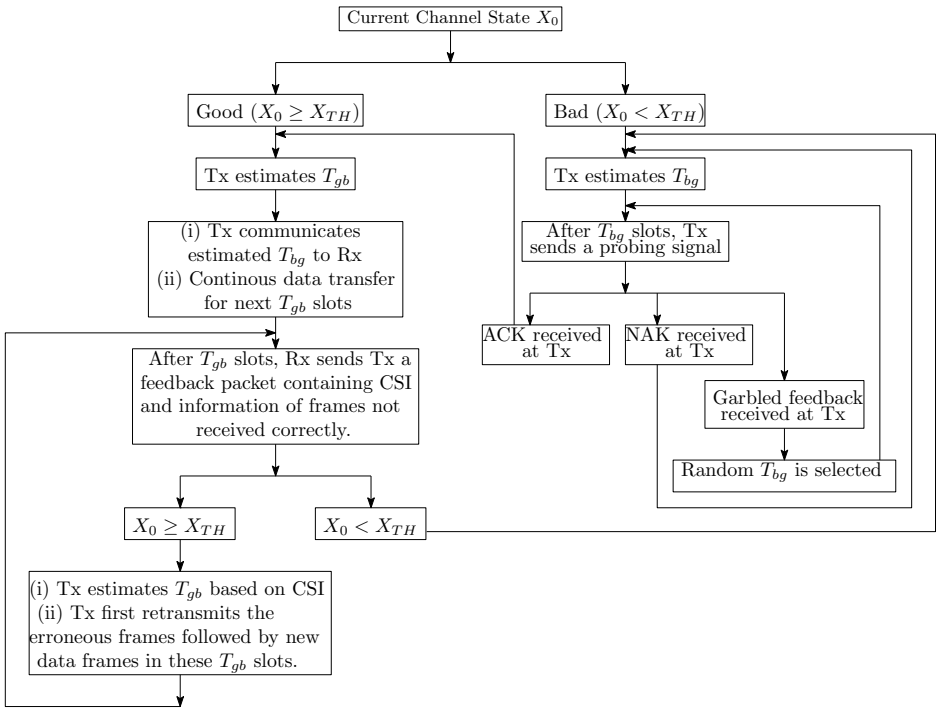

Fig. 1. Proposed channel-aware Dynamic wIndow Protocol (cDIP).

Assuming block fading scenario [14], [19], we we take data frame length T_f to be of single slot, i.e., $T_f = T_s$. Probe packet and ACK/NAK frames are assumed to be very small compared to the slot duration T_s, i.e., $T_p = \kappa T_s$ ($\kappa \ll 1$) [19].

It may also be noted that cDIP is also applicable in a multi-access scenario. When the concerned Tx-Rx link condition is not suitable for data transfer, Tx estimates $\boldsymbol{T_{bg}}$ after which it resumes communication over this link. During this $\boldsymbol{T_{bg}}$ period Tx can cater to the other receivers. With respect to a particular Tx-Rx pair, usage of channel resource during the estimated $\boldsymbol{T_{bg}}$ period is of no consequence. Hence, for our link-layer performance study in this paper we do not include this $\boldsymbol{T_{bg}}$ time usage aspect.

Remark 1. *It is interesting to note that cDIP can be called a combination of channel-aware SW [20] and SR depending on the channel condition. When the channel is in 'bad' state, as in [20], cDIP waits for $\boldsymbol{T_{bg}}$ until the channel becomes usable. On the other hand, when in 'good' state, as in SR, Tx continuously transmits data frames for $\boldsymbol{T_{gb}}$ without waiting for an ACK/NAK. However, unlike in classical SR, only NAK packets are sent for the incorrectly received data packets, which are retransmitted by the Tx.*

III. Stochastic Analysis of Wireless Channel

Noncoherent demodulation [40] is considered at Rx, which is motivated by its simple structure - suitable for low-cost IoT devices. The complex received signal at Rx is $R(t) = R_I(t) + jR_Q(t)$, where $j = \sqrt{-1}$. $R_I(t)$ and $R_Q(t)$ represent the mutually independent quadrature components. At time instant t, received signal envelope at Rx is $X(t) \triangleq |R(t)| = \sqrt{R_I^2(t) + R_Q^2(t)}$. The probability distribution of $X(t)$, i.e., $f_X(x)$ depends on the considered fading model. However, the time derivative of $X(t)$, i.e., $\dot{X}(t) \triangleq \dfrac{dX(t)}{dt} = \lim_{\Delta t \to 0} \dfrac{X(t+\Delta t) - X(t)}{\Delta t}$ is a zero mean Gaussian random variable (RV) irrespective of the underlying distribution of the fading channel, i.e., $\dot{X}(t) \sim \mathcal{N}(0, \dot{\sigma})$ [41].

A. Single Slot Analysis

Using $\dot{X}$ (index t is removed for brevity), we now estimate the probability of SSI staying above X_{TH} (threshold) in the next slot given that it is presently greater than X_{TH}.

Without loss of generality, let us assume SSI at time t is $X(t) = X_{h0}$ and $X_{h0} > X_{TH}$. We obtain SSI in the next time slot by Taylor series expansion as

$$\begin{aligned} X(t+T_s) &= X(t) + \dot{X} \cdot T_s + \ddot{X} \cdot \frac{T_s^2}{2!} + \cdots \\ &\approx X(t) + \dot{X} \cdot T_s \end{aligned} \tag{2}$$

since $T_s \ll 1$. Accordingly, probability that X will continue to remain in 'good' state in next slot is

$$\Pr\{X(t+T_s) \geq X_{TH}\} \overset{\text{by (2)}}{\approx} \Pr\{X_{h0} + X_{h1} \geq X_{TH}\} \tag{3}$$

where $X_{h1}\left(= \dot{X} \cdot T_s\right)$ is a RV denoting temporal variation of the signal envelope in the immediate next slot. Thus, we have $X_{h1} \sim \mathcal{N}(0, \dot{\sigma}_1)$ where $\dot{\sigma}_1 = T_s \dot{\sigma}$. As X_{h1} follows a Gaussian probability distribution, it implies that $X_{h1} \in (-\infty, \infty)$. However, it can be noted that X is SSI, and hence $X_{h0} + X_{h1} \geq 0$, i.e., $X_{h1} \in [-X_{h0}, \infty)$. In other words, X_{h1} actually follows a truncated Gaussian distribution with the following distribution

function:

$$f_{X_{h1}}(\delta) = \begin{cases} \frac{1}{1-\Phi_1\left(-\frac{X_{h0}}{\dot{\sigma_1}}\right)} \frac{1}{\sqrt{2\pi}\dot{\sigma_1}} e^{\left(\frac{-\delta^2}{2\dot{\sigma_1}^2}\right)} & -X_{h0} \leq \delta \\ 0 & \text{elsewhere.} \end{cases} \quad (4)$$

Here $\Phi_1(x) = \int_{-\infty}^{x} \frac{1}{\sqrt{2\pi}} e^{-\frac{t^2}{2}} dt$ is the cumulative distribution function of standard univariate normal distribution and $\dot{\sigma_1}$ depends on the underlying fading model. Using (4) in (3), we get

$$\begin{aligned} \Pr\{X_{h0} + X_{h1} \geq X_{TH}\} &= \int_{X_{TH}-X_{h0}}^{\infty} f_{X_{h1}}(\delta) d\delta \\ &= \frac{1 - \Phi_1\left(\frac{X_{TH}-X_{h0}}{\dot{\sigma_1}}\right)}{1 - \Phi_1\left(-\frac{X_{h0}}{\dot{\sigma_1}}\right)}. \end{aligned} \quad (5)$$

B. Multi-slot Analysis

In continuation from the last section, probability that X will continue to remain above X_{TH} in next two time slots is:

$$\begin{aligned} &\Pr\{X(t+T_s) \geq X_{TH}, X(t+2T_s) \geq X_{TH}\} \\ &\overset{\text{by (3)}}{\approx} \Pr\{X_{h0} + X_{h1} \geq X_{TH}, X_{h0} + X_{h2} \geq X_{TH}\}. \end{aligned} \quad (6)$$

Here X_{h2}, like X_{h1}, is a zero mean truncated Gaussian RV with $\dot{\sigma}_2^2 = 2\dot{\sigma}_1^2$. X_{h2} denotes temporal variation of X over next two slots.

Likewise, probability that X will continue to remain above X_{TH} in next α time slots is:

$$\begin{aligned} &\Pr\{X(t+T_s) \geq X_{TH}, \cdots, X(t+\alpha T_s) \geq X_{TH}\} \\ &\overset{\text{by (3)}}{\approx} \Pr\{X_{h0} + X_{h1} \geq X_{TH}, \cdots, X_{h0} + X_{h\alpha} \geq X_{TH}\}, \end{aligned} \quad (7)$$

where $X_{h\alpha}$ is a zero mean truncated Gaussian RV and $\dot{\sigma}_\alpha^2 = \alpha\dot{\sigma}_1^2$. In general, $X_{h1} \not\perp\!\!\!\perp X_{h2} \not\perp\!\!\!\perp \cdots \not\perp\!\!\!\perp X_{h\alpha}$, and hence $\Pr\{X_{h0} + X_{h1} \geq X_{TH}, \cdots, X_{h0} + X_{h\alpha} \geq X_{TH}\} \neq \prod_{i=1}^{\alpha} \Pr\{X_{h0} + X_{hi} \geq X_{TH}\}$. Therefore, in order to determine the probability (7), we require the joint distribution function $f_{\underline{X_\alpha}}(\underline{x_\alpha}, \Sigma, \underline{X_{\alpha 0}})$ to be integrated over appropriate limits, i.e.,

$$\begin{aligned} &\Pr\{X_{h0} + X_{h1} \geq X_{TH}, \cdots, X_{h0} + X_{h\alpha} \geq X_{TH}\} \\ &= \int_{X_{TH}-X_{h0}}^{\infty} \cdots \int_{X_{TH}-X_{h0}}^{\infty} f_{\underline{X_\alpha}}(\underline{x_\alpha}, \Sigma, \underline{X_{\alpha 0}}) d\underline{x_\alpha}. \end{aligned} \quad (8)$$

Here $f_{\underline{X_\alpha}}(\underline{x_\alpha}, \Sigma, \underline{X_{\alpha 0}})$ is the α-variate truncated Gaussian distribution [42] given by:

$$f_{\underline{X_\alpha}}(\underline{x_\alpha}, \Sigma, \underline{X_{\alpha 0}}) = \frac{e^{-\frac{1}{2}\underline{x_\alpha}^T \Sigma^{-1} \underline{x_\alpha}}}{\int_{\underline{X_{\alpha 0}}}^{\infty} e^{-\frac{1}{2}\underline{x_\alpha}^T \Sigma^{-1} \underline{x_\alpha}} d\underline{x_\alpha}}; \quad \underline{x_\alpha} \in \mathbb{R}^{\alpha}_{\geq \underline{X_{\alpha 0}}} \quad (9)$$

where $\underline{X_\alpha} = [X_{h1}, X_{h2}, \cdots, X_{h\alpha}]^T$ is an α-dimensional random variable, Σ is the $\alpha \times \alpha$ positive definite covariance matrix of $\underline{X_\alpha}$, $\underline{X_{\alpha 0}} = -X_{h0}[\underbrace{1, 1, \cdots, 1}_{\alpha \text{ times}}]^T$, $\mathbb{R}^{\alpha}_{\geq \underline{X_{\alpha 0}}} = \left\{\underline{x_\alpha} \in \mathbb{R}^{\alpha} : \underline{x_\alpha} \geq \underline{X_{\alpha 0}}\right\}$, and $\int_{\underline{X_{\alpha 0}}}^{\infty}$ is an α-dimensional Riemann integral from $\underline{X_{\alpha 0}}$ to ∞. We solve the integral in (8) using the algorithm proposed in [43] for the computation of multivariate Gaussian probabilities.

When $X_{h0} > X_{TH}$, (7) calculates the probability that X will continue to remain above X_{TH} in next α slots. Alternatively it can be said that X will 'cross over' X_{TH} within these α slots with a probability of $1 - \Pr\{X(t+T_s) \geq X_{TH}, \cdots, X(t+\alpha T_s) \geq X_{TH}\}$. Hence this quantity is defined as the 'level crossing probability'. It is interesting to note that irrespective of the underlying fading distribution, (7) is always computed by integrating a scaled multi-variate Gaussian distribution, i.e., the level crossing probability is independent of the channel fading distribution.

C. CTI Estimation

Based on the analysis presented in Section III-B, we propose a *Continuous Transmission Interval (CTI)* estimation scheme. The estimated CTI $\boldsymbol{T_{gb}}$ gives us an idea about the time the channel will continue to remain suitable for data transmission given that it is currently suitable. If estimated CTI $= \alpha_{gb}$ slots, then the actual time interval is $\boldsymbol{T_{gb}} = \alpha_{gb} T_s$ sec. This CTI has been used in our proposed protocol operation.

In CTI estimation it can be stated that given X_{h0}, we are interested in estimating the time for which X will continue to remain in 'good' state ($X \geq X_{TH}$) before reaching the 'bad' state, i.e., $X < X_{TH}$. It may be noted that α_{gb} is *probabilistic* based on *level crossing probability* ϵ. Lesser the value of ϵ, the more sure we are about the calculated value of α_{gb}.

With energy-efficient data communication being a key objective, we intend to reduce the unnecessary wastage of both time and energy due to the transmission of ACKs for each data frame. This allows seamless data frame transmission over the next α_{gb} slots during which interval $X \geq X_{TH}$ with very high probability $1 - \epsilon$.

Accordingly we calculate α_{gb}^* (optimal value of α_{gb}) for a given set of system parameters (f_D and T_s), X_{h0}, X_{TH}, and ϵ by solving the optimization problem P1.

$$\text{(P1)} \quad : \underset{\alpha_{gb} \geq 0}{\text{maximize}} \ \alpha_{gb} \quad (10)$$

subject to

$$\Pr\left\{X_{h0} + X_{h1} \geq X_{TH}, \cdots, X_{h0} + X_{h\alpha_{gb}} \geq X_{TH}\right\} \geq 1 - \epsilon.$$

$\Pr\left\{X_{h0} + X_{h1} \geq X_{TH}, \cdots, X_{h0} + X_{h\alpha_{gb}} \geq X_{TH}\right\}$ in P1 is calculated as described in Section III-B.

Lemma 1. *[22, Lemma 1] If $X_0 < X_{TH}$, then we have*

$$\lim_{N \to \infty} \Pr\{X_0 + X_1 < X_{TH}, \cdots, X_0 + X_N < X_{TH}\} = 0. \quad (11)$$

Here X_1 like X_{h1} is a zero mean truncated Gaussuan RV in $[-X_0, \infty)$ with variance $\dot{\sigma}_1$. Similarly, X_N is also a zero mean truncated Gaussian RV, but with $\dot{\sigma}_N^2 = N\dot{\sigma}_1^2$.

Remark 2. *For a given set of system parameters, $\{g_n\}$ is a Cauchy sequence, where*

$$g_n = \Pr\{X_{h0} + X_{h1} \geq X_{TH}, \cdots, X_{h0} + X_{hn} \geq X_{TH}\}.$$

A sequence $\{x_n\}$ is said to be a Cauchy sequence [44] if $\forall\ \Gamma > 0,\ \exists\ n_0 \in \mathbb{N}$ such that

$$|x_n - x_m| < \Gamma \quad \forall\ n, m \geq n_0. \tag{12}$$

As g_n is a probability, $g_n \in [0, 1]$. Moreover from Lemma 1, we can prove that

$$\lim_{n\to\infty} \Pr\{X_{h0} + X_{h1} \geq X_{TH}, \cdots, X_{h0} + X_{hn} \geq X_{TH}\} = 0. \tag{13}$$

Thus it can be observed that $\{g_n\} \downarrow 0$, i.e., $\{g_n\}$ is a monotonically decreasing sequence with $\lim_{n\to\infty} g_n = 0$. We know from [45, Theorem 3.11(a)] that every convergent sequence is a Cauchy sequence. Hence $\{g_n\}$ is a Cauchy sequence.

It can be noted that solving P1 requires integration over α-variate truncated Gaussian distributions, with α starting from 1 and increasing in each step till the solution is obtained. This sequential method of solving P1 over $\mathbb{N}$ is not efficient, its computational complexity being $O(n)$. Hence using $\{g_n\} \downarrow 0$, we reformulate P1 accordingly to propose a minimal complexity algorithm for obtaining α^*_{gb}.

Before introducing the algorithm, we define the lower bound α^l_{gb} and upper bound α^u_{gb} respectively of α_{gb}, for a given set of X_{h0}, X_{TH}, f_D, T_s, and ϵ.

1) α^l_{gb} is calculated by considering complete independence among the X_{hi}'s, i.e.,

$$\begin{aligned}&\Pr\left\{X_{h0} + X_{h1} \geq X_{TH}, \cdots, X_{h0} + X_{h\alpha_{gb}} \geq X_{TH}\right\} \\ &= \prod_{i=1}^{\alpha_{gb}} \Pr\{X_{h0} + X_{hi} \geq X_{TH}\} = \prod_{i=1}^{\alpha_{gb}} \frac{1 - \Phi_1\left(\frac{X_{TH} - X_{h0}}{\dot{\sigma_i}}\right)}{1 - \Phi_1\left(-\frac{X_{h0}}{\dot{\sigma_i}}\right)},\end{aligned} \tag{14}$$

where X_{hi} is a zero mean truncated Gaussian RV with $\sigma_i^2 = i\sigma_1^2$. Accordingly we obtain α^l_{gb} as:

$$\begin{aligned}&\text{(P2)} \quad : \underset{\alpha_{gb} \geq 0}{\text{maximize}}\ \alpha_{gb} \\ &\text{subject to} \quad \prod_{i=1}^{\alpha_{gb}} \frac{1 - \Phi_1\left(\frac{X_{TH} - X_{h0}}{\dot{\sigma_i}}\right)}{1 - \Phi_1\left(-\frac{X_{h0}}{\dot{\sigma_i}}\right)} \geq 1 - \epsilon.\end{aligned} \tag{15}$$

2) α^u_{gb} is calculated based on the probability of X crossing X_{TH} in the α^u_{gb}th slot irrespective of whether it had crossed X_{TH} before or not. Hence we obtain α^u_{gb} as:

$$\begin{aligned}&\text{(P3)} \quad : \underset{\alpha_{gb} \geq 0}{\text{maximize}}\ \alpha_{gb} \\ &\text{subject to} \quad \frac{1 - \Phi_1\left(\frac{X_{TH} - X_{h0}}{\dot{\sigma}_{\alpha_{gb}}}\right)}{1 - \Phi_1\left(-\frac{X_{h0}}{\dot{\sigma}_{\alpha_{gb}}}\right)} \geq 1 - \epsilon.\end{aligned} \tag{16}$$

As $\epsilon \geq 0$, with α^l_{gb} and α^u_{gb} estimated we reformulate P1 into an optimization problem with an unimodal objective function. Thus we reformulate (10) as:

$$\begin{aligned}\text{(P4)} : \alpha^*_{gb} = \Bigg\{\alpha_{gb} \mid \underset{\alpha^l_{gb} \leq \alpha_{gb} \leq \alpha^u_{gb}}{\text{argmin}} \big[\Pr\{X_{h0} + X_{h1} \geq X_{TH}, \cdots \\ \cdots, X_{h0} + X_{h\alpha_{gb}} \geq X_{th}\} - (1 - \epsilon)\big]^2\Bigg\}.\end{aligned} \tag{17}$$

The objective function in P4 is unimodal with the optimum achieved when $1 - \epsilon = g_{\alpha_{gb}}$. Due to this unimodal nature of the objective function, the local minima obtained in this context is itself the global minima. Accordingly, we propose Algorithm 1 using golden section based line search method [46] to obtain α^*_{gb}. Convergence properties of golden section method are proved in [47].

Algorithm 1 Algorithm to find α^*_{gb}

Require: X_{TH}, X_{h0}, f_D, T_s, ϵ, and $\xi > 0$
Ensure: α^*_{gb}
Calculate α^l_{gb} using (15) and α^u_{gb} using (16)
Define $r(\alpha) = [\Pr\{X_{h0} + X_{h1} \geq X_{TH}, \cdots \cdots, X_{h0} + X_{h\alpha} \geq X_{TH}\} - (1 - \epsilon)]^2$
Set $k = 0$
Calculate $\alpha_p = \alpha^u_{gb} - 0.618 \times (\alpha^u_{gb} - \alpha^l_{gb})$
Calculate $\alpha_q = \alpha^l_{gb} + 0.618 \times (\alpha^u_{gb} - \alpha^l_{gb})$
Calculate $r(\alpha_p)$ and $r(\alpha_q)$
Set $\Delta_{gb} = \alpha^u_{gb} - \alpha^l_{gb}$
while $\Delta_{gb} > \xi$ **do**
  if $r(\alpha_p) \leq r(\alpha_q)$ **then**
    Set $\alpha^u_{gb} = \alpha_q$, $\alpha_q = \alpha_p$, and $\alpha_p = \alpha^u_{gb} - 0.618 \times (\alpha^u_{gb} - \alpha^l_{gb})$
  else
    Set $\alpha^l_{gb} = \alpha_p$, $\alpha_p = \alpha_q$, and $\alpha_q = \alpha^l_{gb} + 0.618 \times (\alpha^u_{gb} - \alpha^l_{gb})$
  end if
  Set $k = k + 1$
  Calculate $r(\alpha_p)$ and $r(\alpha_q)$
  Set $\Delta_{gb} = \alpha^u_{gb} - \alpha^l_{gb}$
end while
if $r(\alpha_p) < r(\alpha_q)$ **then**
  Set $\alpha^*_{gb} = \alpha_p$
else
  Set $\alpha^*_{gb} = \alpha_q$
end if

D. CWI Estimation

If the current SSI $X(t) = X_{l0} (< X_{TH})$ and estimated continuous waiting interval (CWI) $\boldsymbol{T_{bg}}$ gives us an idea about the duration the channel will continue to remain in $X < X_{TH}$ region, then $\boldsymbol{T_{bg}} = \alpha_{bg} T_s$ sec. Here α^*_{bg} (optimal α_{bg}) for a given set of system parameters is obtained by solving:

$$\begin{aligned}&\text{(P5)} \quad : \underset{\alpha_{bg} \geq 0}{\text{maximize}}\ \alpha_{bg} \\ &\text{subject to} \\ &\Pr\left\{X_{l0} + X_{l1} < X_{TH}, \cdots, X_{l0} + X_{l\alpha_{bg}} < X_{TH}\right\} \geq 1 - \epsilon.\end{aligned} \tag{18}$$

Similarly as X_{hi} (presented in Section III-B), X_{li} is also a truncated Gaussian RV with $\dot{\sigma}_i^2 = i\dot{\sigma}_1^2$, where

$$f_{X_{l1}}(\delta) = \begin{cases} \frac{1}{1 - \Phi_1\left(-\frac{X_{l0}}{\dot{\sigma}_1}\right)} \frac{1}{\sqrt{2\pi}\dot{\sigma}_1} e^{\left(\frac{-\delta^2}{2\dot{\sigma}_1{}^2}\right)} & -X_{l0} \leq \delta \\ 0 & \text{elsewhere.} \end{cases} \tag{19}$$

P5 is solved in the manner similar to P1, i.e., P5 is first reformulated to an optimization problem with unimodal objective function. Then we exploit this unimodal nature of the objective function to obtain α_{bg}^* using golden section based line search method.

Remark 3. *Though the proposed analytical framework is for slotted communication scenario, it can be applied to unslotted scenarios as well. It is just that with time slot granularity of T_s secs, the estimated CTIs and CWIs are interpreted in terms of number of slots. The system can be considered virtually operating in unslotted mode if the chosen T_s is sufficiently smaller than the typical CTI or CWI.*

Given the estimate of $\boldsymbol{T_{gb}}$ and $\boldsymbol{T_{bg}}$, through the following Theorem 1 we establish a relation between these two quantities.

Theorem 1. *For a given set of system parameters, i.e., f_D, T_s, and ϵ, we always have $\boldsymbol{T_{gb}} \geq \boldsymbol{T_{bg}}$ when $X_{h0} - X_{TH} = X_{TH} - X_{l0}$.*

Proof: Let $X_{h0} - X_{TH} = X_{TH} - X_{l0} \triangleq \gamma$.

From (4) and (19), we have

$$\Pr\{X_{h0} + X_{h1} \geq X_{TH}\} = \frac{1}{1 - \Phi_1\left(-\frac{X_{h0}}{\dot{\sigma_1}}\right)} \int_{X_{TH}-X_{h0}}^{\infty} \frac{1}{\sqrt{2\pi}\dot{\sigma_1}} e^{\left(\frac{-\delta^2}{2\dot{\sigma_1}^2}\right)} d\delta, \quad \text{and}$$

$$\Pr\{X_{l0} + X_{l1} < X_{TH}\} = \frac{1}{1 - \Phi_1\left(-\frac{X_{l0}}{\dot{\sigma_1}}\right)} \int_{-X_{l0}}^{X_{TH}-X_{l0}} \frac{1}{\sqrt{2\pi}\dot{\sigma_1}} e^{\left(\frac{-\beta^2}{2\dot{\sigma_1}^2}\right)} d\beta$$

respectively. Hence,

$$\frac{\Pr\{X_{h0} + X_{h1} \geq X_{TH}\}}{\Pr\{X_{l0} + X_{l1} < X_{TH}\}} = \frac{\frac{1}{1 - \Phi_1\left(-\frac{X_{h0}}{\dot{\sigma_1}}\right)} \int_{X_{TH}-X_{h0}}^{\infty} \frac{1}{\sqrt{2\pi}\dot{\sigma_1}} e^{\left(\frac{-\delta^2}{2\dot{\sigma_1}^2}\right)} d\delta}{\frac{1}{1 - \Phi_1\left(-\frac{X_{l0}}{\dot{\sigma_1}}\right)} \int_{-X_{l0}}^{X_{TH}-X_{l0}} \frac{1}{\sqrt{2\pi}\dot{\sigma_1}} e^{\left(\frac{-\beta^2}{2\dot{\sigma_1}^2}\right)} d\beta} \tag{20}$$

$$= A(\gamma) \times B(\gamma), \text{ where } A(\gamma) = \frac{1 - \Phi_1\left(-\frac{X_{l0}}{\dot{\sigma_1}}\right)}{1 - \Phi_1\left(-\frac{X_{h0}}{\dot{\sigma_1}}\right)}$$

and $B(\gamma) = \dfrac{\int_{X_{TH}-X_{h0}}^{\infty} \frac{1}{\sqrt{2\pi}\dot{\sigma_1}} e^{\left(\frac{-\delta^2}{2\dot{\sigma_1}^2}\right)} d\delta}{\int_{-X_{l0}}^{X_{TH}-X_{l0}} \frac{1}{\sqrt{2\pi}\dot{\sigma_1}} e^{\left(\frac{-\beta^2}{2\dot{\sigma_1}^2}\right)} d\beta}$.

Rewriting $A(\gamma)$ in terms of X_{TH}, we obtain $A(\gamma) = \dfrac{1 - \Phi_1\left(\frac{-X_{TH}+\gamma}{\dot{\sigma_1}}\right)}{1 - \Phi_1\left(\frac{-X_{TH}-\gamma}{\dot{\sigma_1}}\right)}$. Since $\dot{\sigma}_1 = T_s\dot{\sigma}$ and T_s is practically on the order of μsec, i.e., $T_s \ll 1$, we can approximate $A(\gamma) \approx 1$. $B(\gamma)$ is obtained as follows:

$$B(\gamma) = \frac{\int_{X_{TH}-X_{h0}}^{\infty} \frac{1}{\sqrt{2\pi}\dot{\sigma_1}} e^{\left(\frac{-\delta^2}{2\dot{\sigma_1}^2}\right)} d\delta}{\int_{-X_{l0}}^{X_{TH}-X_{l0}} \frac{1}{\sqrt{2\pi}\dot{\sigma_1}} e^{\left(\frac{-\beta^2}{2\dot{\sigma_1}^2}\right)} d\beta} \overset{(a)}{=} \frac{\int_{-\gamma}^{\infty} \frac{1}{\sqrt{2\pi}\dot{\sigma_1}} e^{\left(\frac{-\delta^2}{2\dot{\sigma_1}^2}\right)} d\delta}{\int_{-\infty}^{\gamma} \frac{1}{\sqrt{2\pi}\dot{\sigma_1}} e^{\left(\frac{-\beta^2}{2\dot{\sigma_1}^2}\right)} d\beta - \int_{-\infty}^{-X_{TH}+\gamma} \frac{1}{\sqrt{2\pi}\dot{\sigma_1}} e^{\left(\frac{-\beta^2}{2\dot{\sigma_1}^2}\right)} d\beta} \overset{(b)}{\geq} 1. \tag{21}$$

Here (a) is obtained by the changing of limits, as $X_{h0} - X_{TH} = X_{TH} - X_{l0} = \gamma$. Moreover, by inspection $\int_{-\gamma}^{\infty} \frac{1}{\sqrt{2\pi}\dot{\sigma_1}} e^{\left(\frac{-\delta^2}{2\dot{\sigma_1}^2}\right)} d\delta$ and $\int_{-\infty}^{\gamma} \frac{1}{\sqrt{2\pi}\dot{\sigma_1}} e^{\left(\frac{-\beta^2}{2\dot{\sigma_1}^2}\right)} d\beta$ are identical as both involve a zero mean Gaussian random variable with same variance. Hence, $\int_{-\infty}^{-X_{TH}+\gamma} \frac{1}{\sqrt{2\pi}\dot{\sigma_1}} e^{\left(\frac{-\beta^2}{2\dot{\sigma_1}^2}\right)} d\beta$ being non-negative, (b) follows.

Thus we get $\dfrac{\Pr\{X_{h0} + X_{h1} \geq X_{TH}\}}{\Pr\{X_{l0} + X_{l1} < X_{TH}\}} \geq 1$. Since $\dot{\sigma_i}^2 = i\dot{\sigma_1}^2 \ \forall \ i \in \mathbb{Z}^+$, (20) can be generalized as $\dfrac{\Pr\{X_{h0} + X_{h1} \geq X_{TH}, \cdots, X_{h0} + X_{hi} \geq X_{TH}\}}{\Pr\{X_{l0} + X_{l1} < X_{TH}, \cdots, X_{l0} + X_{li} < X_{TH}\}} \geq 1 \quad \forall\, i$. In other words, $\boldsymbol{T_{gb}} \geq \boldsymbol{T_{bg}}$ for a given set of system parameters and this completes the proof. □

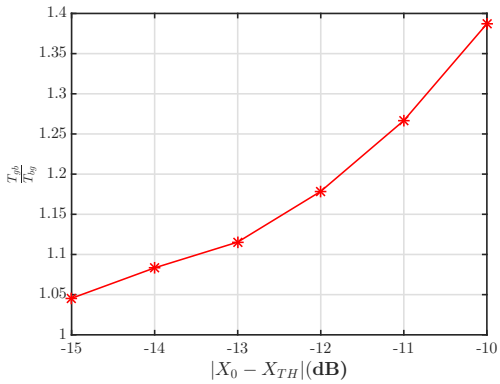

Fig. 2. Variation of $\frac{\boldsymbol{T_{gb}}}{\boldsymbol{T_{bg}}}$ versus $|X_0 - X_{TH}|$.

Numerical verification of the proof has been presented in Fig. 2. In this figure, we show that $\frac{\boldsymbol{T_{gb}}}{\boldsymbol{T_{bg}}} \geq 1$, i.e., $\boldsymbol{T_{gb}} \geq \boldsymbol{T_{bg}}$ against $|X_0 - X_{TH}|$ when an unit power signal is transmitted

over a Rayleigh fading channel with fading margin $F = 10$dB, $v = 12$ kmph, and $T_s = 200$ μsec. The overall increasing trend of $\frac{\boldsymbol{T_{gb}}}{\boldsymbol{T_{bg}}}$ with $|X_0 - X_{TH}|$ is also to be noted in the figure.

Remark 4. *Thus, we can state from Theorem* 1 *that when the channel is in very 'good' state, it will continue to stay in the 'good' state for a relatively longer amount of time compared to the time duration it stays in 'bad' state given that it is currently in deep fade state such that* $X_{TH} - X_{l0} = X_{h0} - X_{TH}$.

This non-intuitive result signifies the importance of the current channel state in data communication, noted in the proposed cDIP performance, presented next.

Remark 5. *From the analysis in Section III it is apparent that, estimation of* $\boldsymbol{T_{gb}}$ *and* $\boldsymbol{T_{bg}}$ *are dependent on* $f_{\dot{X}}(\dot{x})$*, i.e., the distribution of rate of temporal variation of the channel only; it is agnostic to the distribution of the underlying channel fading distribution.*

IV. Performance Analysis of cDIP

In this section we quantify the performance of cDIP in terms of data throughput and energy efficiency. Then we formulate an optimization problem that maximizes energy efficiency for a given set of system parameters by calculating the optimal ϵ.

A. Performance Measures

The different performance measures are defined as follows:

Definition 1. *Data throughput* D_T *is the long-term average of successfully delivered data frames per second.*

Accordingly we obtain:

$$D_T = \frac{\frac{(1-\epsilon)}{\zeta}\overline{\alpha_{gb}}}{(\overline{\alpha_{gb}} + \overline{\alpha_{bg}})T_s + 3T_p} \quad \text{frames/sec}, \tag{22}$$

where ζ is the interval between two consecutive data frame transmission attempts. $\overline{\alpha_{gb}}$ and $\overline{\alpha_{bg}}$ are long-term averages of α_{gb} and α_{bg} respectively, i.e., $\overline{\alpha_{gb}} = \lim_{N\to\infty} \frac{1}{N} \sum_{i=1}^{N} \alpha_{gb}(i)$, $\overline{\alpha_{bg}} = \lim_{N\to\infty} \frac{1}{N} \sum_{i=1}^{N} \alpha_{bg}(i)$, and the factor $3T_p$ accounts for the time period due to probing based three way handshake between Rx and Tx.

Definition 2. *A complete cycle is the duration between two consecutive CTIs. Thus a complete cycle includes a CTI* $\overline{\alpha_{gb}}$*, followed by an ACK/NAK from Rx, a CWI* $\overline{\alpha_{bg}}$*, and a probing handshake between Rx and Tx, after which another CTI begins.*

Definition 3. *Energy consumption* E_C *is the long-term average consumption per successful data frame delivery.*

In other words, E_C is the energy consumption per complete cycle for each successfully delivered data frame, i.e.,

$$E_C = \frac{\frac{\overline{\alpha_{gb}}}{\zeta}\varepsilon_f + 2\varepsilon_a + \varepsilon_p + (\overline{\alpha_{gb}} + \overline{\alpha_{bg}})\varepsilon_w}{\frac{(1-\epsilon)}{\zeta}\overline{\alpha_{gb}}} \quad \text{Joules} \tag{23}$$

where $\varepsilon_f, \varepsilon_a$, and ε_p, denote transmit and receive energy respectively per data frame, ACK/NAK frame, and probing frame, and ε_w is the energy consumption in idle state, i.e., circuit energy consumption per idle time slot. The term $\frac{\overline{\alpha_{gb}}}{\zeta}\varepsilon_f$ corresponds to energy consumption during CTI, ε_a corresponds to the ACK/NAK from Rx, $(\varepsilon_p + \varepsilon_a)$ is due to the handshaking between Rx and Tx, and $(\overline{\alpha_{gb}} + \overline{\alpha_{bg}})\varepsilon_w$ is the energy consumption in this entire duration. $\varepsilon_f, \varepsilon_a, \varepsilon_p$, and ε_w are defined as:

$$\varepsilon_f = T_f\left(I_t^2 + I_r^2\right)R,\ \ \varepsilon_a = T_p\left(I_t^2 + I_r^2\right)R,\ \ \varepsilon_w = 2I_w^2 T_f R,$$
$$\text{and} \quad \varepsilon_p = 2T_p\left(I_t^2 + I_r^2\right)R + 2\left(T_f - 2T_p\right)I_w^2 R \tag{24}$$

where I_t, I_r, and I_w are the current consumptions in transmission, reception, and waiting modes respectively, with R being the circuit resistance.

Remark 6. *Note that the energy consumption in idle state is accounted for entire* $(\overline{\alpha_{gb}} + \overline{\alpha_{bg}})$ *and not only* $\overline{\alpha_{gb}}$*. This is because, even with the IoT node not transmitting during* $\overline{\alpha_{bg}}$*, a very small fraction of its energy continues to drain out. The node virtually is in 'sleep' state during this period but not totally 'off', much like the discontinuous reception/transmission (DRX/DTX) mechanism of LTE-A [35].*

It is intuitive that a higher energy consumption may result in a higher data throughput. This tradeoff is efficiently captured by the performance metric of '*energy efficiency*'.

Definition 4. *Energy efficiency* η *is defined as [48]:*

$$\eta = \frac{D_T}{E_C} \quad \textit{frames/sec/Joule}. \tag{25}$$

B. Optimal ϵ for Energy Efficiency Maximization

Since D_T and E_C are functions of level crossing probability ϵ, η is also a function of ϵ. Here we estimate the optimal ϵ that maximizes η for a given set of system parameters.

ϵ is in range $[0, 1]$. ϵ being an application dependent parameter, it is the application at hand that specifies an acceptable tighter range of ϵ. Accordingly we introduce an user-defined range of ϵ, i.e., $\epsilon \in [\epsilon_l, \epsilon_u]$ and formulate an optimization problem to obtain ϵ^* (optimal ϵ) as follows:

$$(\text{P6}) : \epsilon^* = \left\{ \epsilon \;\middle|\; \underset{\epsilon_l \le \epsilon \le \epsilon_u}{\operatorname{argmax}}\, \eta \right\}. \tag{26}$$

With ϵ^* known, the corresponding η is calculated using (25).

Before concluding the section, we briefly discuss the existing competitive approaches, namely, adaptive probing variants (AP1, AP2) and coherence time based waiting (CT):

1) AP1 [20]: This scheme proposes to take *average fade duration* (AFD) as $\boldsymbol{T_{bg}}$.

   AFD for a given threshold X_{TH} is defined as [49]:

   $$\rho_{X_{TH}} = \frac{\Pr\{X < X_{TH}\}}{\int_0^\infty \dot{x} f_{X,\dot{X}}(X_{TH}, \dot{x}) d\dot{x}}, \tag{27}$$

   where $f_{X,\dot{X}}(x, \dot{x})$ is the joint probability distribution of X and $\dot{X}$. AFD in terms of slots is $\rho_{\text{slots}} = \left\lceil \frac{\rho_{X_{TH}}}{T_s} \right\rceil$.
2) AP2 [20]: It proposes $\boldsymbol{T_{bg}} = \left\lceil \frac{0.5 \times (\rho_{X_{TH}} - \rho_{X_i})}{T_s} \right\rceil$, where $X_i = X_p + \frac{X_{TH}}{2N}$ is the quantized SSI in $\{X_p, X_{p+1}\}$

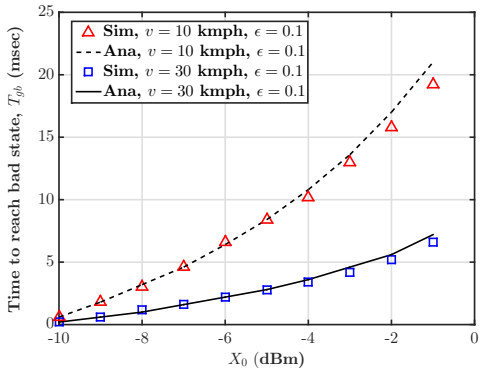

Fig. 3. Verification of $\boldsymbol{T_{gb}}$ estimation. $X_{TH} = -10.4576$ dBm.

when $[0, X_{TH})$ is quantized into N levels with step size $\frac{X_{TH}}{N}$.

3) CT [21]: This scheme takes coherence time T_C as the default $\boldsymbol{T_{bg}}$ irrespective of current channel state. As defined in [50], we take $T_C = \frac{0.423}{f_D}$ and thus $\boldsymbol{T_{bg}} = \left\lceil \frac{T_C}{T_s} \right\rceil$.

It is important to note that these existing approaches aim at only reducing chances of blind transmission when the channel is in 'bad' state, i.e., they only estimate $\boldsymbol{T_{bg}}$. As a result, they fail to exploit the channel to its fullest when it is in good state. Moreover, in these protocols, for each frame transmission an ACK is required, as in classical ARQ protocols.

V. Numerical Results

In this section, we evaluate cDIP via extensive simulations and also compare its performance with the existing competitive approaches: AP1 [20], AP2 [20], and CT [21].

Results are obtained by considering a unit power signal transmission over Rayleigh fading channel. The acceptable range of ϵ is taken as $\epsilon \in [0, 0.5]$.

The reason behind taking $\epsilon \in [0, 0.5]$ is that by definition $\epsilon \geq 0$ and $\epsilon = 0.5$ implies that there is atleast 50% chance that X will reach above/below X_{TH} in the estimated $\boldsymbol{T_{bg}}/\boldsymbol{T_{gb}}$ given that it is currently below/above X_{TH}. System parameters considered are: carrier frequency $f_c = 900$ MHz, slot duration $T_s = 200$ μs, $\kappa = 0.1$, and $\zeta = 1$. Considering short-range IoT communication, propagation delay is ignored.

A. Verification of $\boldsymbol{T_{gb}}$ Estimation through Simulation

We first compare the analytically estimated $\boldsymbol{T_{gb}}$ with Monte Carlo simulations. Fig. 3 shows that, current state X_0 plays a pivotal role in determining $\boldsymbol{T_{gb}}$. Note that $X_0 \gg X_{TH}$ is not the same as X_0 being just more than X_{TH}; with $v = 10$ kmph, $\epsilon = 0.1$, and $X_{TH} = -10.4576$ dBm, $\boldsymbol{T_{gb}} = 0.0018$ sec for $X_0 = -9$ dBm, whereas $\boldsymbol{T_{gb}} = 0.021$ sec for $X_0 = -1$ dBm.

With Fig. 3 showing that the estimated $\boldsymbol{T_{gb}}$ matches closely with the results obtained through Monte Carlo simulations, it validates cDIP and justifies the role of X_0 in estimating $\boldsymbol{T_{gb}}$. Also it is noted that the rate of increase of $\boldsymbol{T_{gb}}$ with X_0 decreases with increasing node velocity; $\frac{\partial \boldsymbol{T_{gb}}}{\partial X_0} = 0.002267$ and 0.000778 for $v = 10$ and 30 kmph respectively. Another interesting observation is that $\boldsymbol{T_{gb}}$ for a particular X_0 increases with decreasing value of v. The reason behind both these observations is that at a smaller v, channel fading is slower and as a result more time is taken in changing state.

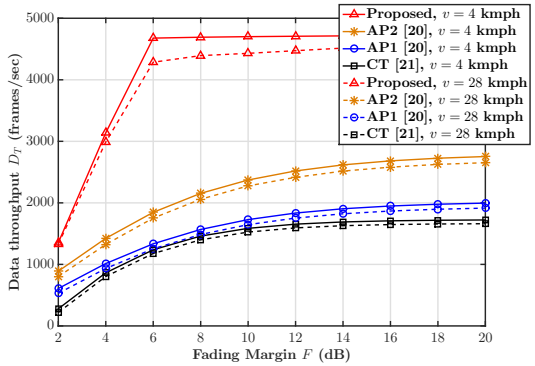

(a) Effect of fading margin on data throughput.

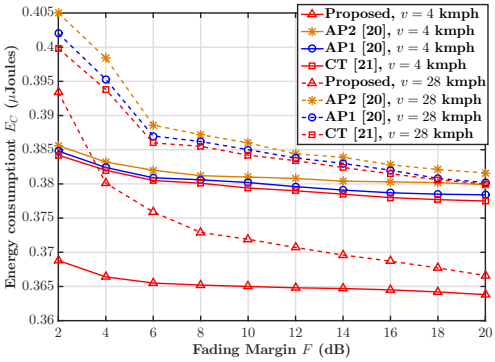

(b) Effect of fading margin on energy consumption.

Fig. 4. Effect of fading margin on performance of cDIP.

B. Effect of Operating Parameters on System Performance

We now discuss the effect of fading margin F [19] on data throughput D_T and energy consumption E_C performance of cDIP. Fig. 4(a) shows that, irrespective of the channel aware transmission approach D_T increases with increase in F. This is intuitive also; channel spends relatively more time in 'good' state with increasing F and this results in an increase in D_T and decrease in E_C. Apart from the above-mentioned trend of D_T against F, it is also noted that cDIP outperforms AP1, AP2, and CT.

AP1, AP2, and CT mainly focused on estimating the waiting interval $\boldsymbol{T_{bg}}$ when channel is not suitable for data transfer. Additionally, all of them require ACK for the individual data frame. cDIP on the other hand also estimates the continuous data transmission interval $\boldsymbol{T_{gb}}$ when the channel is in 'good' state, thus avoiding the requirement of individual ACKs. At the end of $\boldsymbol{T_{gb}}$, Rx sends a feedback packet to TX containing CSI and information of the frames erroneously received. This resulting reduction of overhead in cDIP offers significantly higher D_T; $D_T = 1354$ frames/sec when $F = 2$ dB compared to $D_T = 4740$ frames/sec when $F = 20$ dB.

Fig. 4(b) shows the effect of F on E_C; we observe a decreasing trend in E_C with increasing F. It is also noted that, cDIP outperforms its competitors by a significant margin.

C. Computation Complexity and Overhead

As noted from the analysis in Section III, the modified optimization problem P4 for computation of optimum CTI has logarithmic complexity. Specifically, the proposed algorithm terminates after N_I iterations if

$$(\alpha_{gb}^{u} - \alpha_{gb}^{l}) \times 0.618^{N_I} \leq \chi, \tag{28}$$

where χ is the tolerance level [46], i.e., we obtain $N_I \leq 2\ln\left(\frac{\alpha_{gb}^{u} - \alpha_{gb}^{l}}{\chi}\right)$. Hence, the computation complexity is $O\left(\log\left(\frac{1}{\chi}\right)\right)$.

With the modern processors, having speed on the order of GHz, the optimum CTI/CWI can be performed in μs order of time, which is well within a slot duration T_s. Yet, to alleviate the need for online CTI/CWI estimation, we propose a look-up table-driven CTI/CWI selection approach as shown in Table I.

Table I. Optimal parameters for maximized energy efficiency under different channel conditions with $f_D T_s = 0.002$, and $X_{TH} = -10.4576$ dBm.

X_{h0} (dBm)	α_{gb}^{*} (slots)	X_{l0} (dBm)	α_{bg}^{*} (slots)
-10	2	-11	1
-9	7	-12	3
-8	12	-13	4
-7	18	-14	6
-6	25	-15	7
-5	33	-16	8

Table I consists of optimal parameters (CTI and CWI) corresponding to different channel state values (X_{h0} and X_{l0}), which are computed offline and stored beforehand. This look-up table is used to adapt with the changing X_{h0} and X_{l0}. Table I consists of four entries corresponding to $f_D T_s = 0.002$ and $X_{TH} = -10.4576$ dBm. Both T_s and X_{TH}, being application-specific, are known beforehand. Only f_D varies depending on mobility of the environment. Considering this fact, we propose a generic look-up table for a range of f_D values and not a single value, unlike Table I, consisting of optimal CTI and CWI corresponding to various values of X_{h0} and X_{l0}. The entries in this table, like Table I, are also computed offline and stored beforehand.

For finding the parameters other than the ones present in the table, an IoT node has two options depending on its computational capability: estimate the parameters according to the proposed Algorithm 1 or consider the closest entry in the look-up table. Intuitively, the performance of this approach can be refined by having fine granular entries in the table.

It may also be noted that although cDIP operation mechanism is very similar to the traditional ARQ protocols, its Tx-end channel awareness aspect incurs some additional overhead as in AP2 [20] which is studied in this section. In proposed cDIP, Tx estimates $\boldsymbol{T_{gb}}$ given that the channel is currently usable. Tx sends this information to Rx, which is required for a collective feedback packet to Tx after $\boldsymbol{T_{gb}}$, containing information on the erroneously received data frames. This requires some additional number of bits B_{TX}.

To investigate the effect of this additional overhead on performance of cDIP, energy efficiency η is plotted against

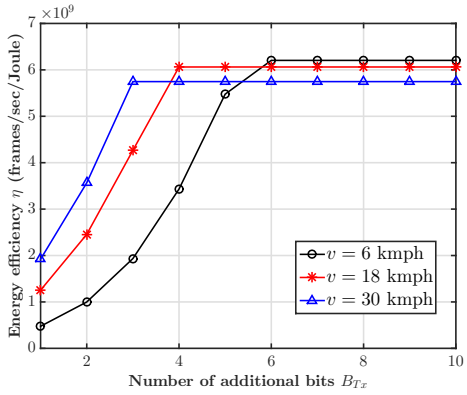

Fig. 5. Effect of overhead B_{TX} on energy efficiency η of cDIP. $\epsilon = 0.05$, and $X_{TH} = -3.9788$ dBm.

B_{TX} in Fig. 5. It is observed that irrespective of the value of v, η initially increases with B_{TX} before saturating beyond a certain point B_{TX}^{saturate}. It is also interesting to note that at a lower node mobility, a higher B_{TX}^{saturate} is required and vice-versa; $B_{TX}^{\text{saturate}} = 6, 4$, and 3 bits for $v = 6, 18$, and 30 kmph respectively. This in a way, reinforces the observation in Fig. 3, where it was observed that for identical channel condition $\boldsymbol{T_{gb}}$ estimated is higher for a lower value of v. Hence a higher number of bits are required to transfer this information to Rx, which results in a higher B_{TX}^{saturate} at lower node velocity. As a result η continues to increase proportionately with increasing B_{TX} till B_{TX}^{saturate}, beyond which η saturates.

However, as discussed in the next subsection, with this small amount of extra overhead a significant gain in system performance is achieved.

D. Protocol Performance Comparison

Here we compare the performance of cDIP in terms of D_T and η, with the ones proposed in [20], [21] that have the closest system settings.

1) Data throughput D_T: Fig. 6(a) exhibits an overall decreasing trend of D_T with v. This implies that, increasing v results in a high $f_D T_s$ product, i.e., the channel is now relatively less correlated than it was with a lower $f_D T_s$. As a result, the channel should be sensed more frequently to estimate its state, which leads to decrease of both D_T and η, and increase of E_C.

Fig. 6(a) demonstrates that AP1 [20] and CT [21] achieve very low D_T with respect to the others. They respectively achieve D_T in the range of 1000 to 1050 and 850 to 900 frames/sec, which is approximately 58% and 64% lesser with respect to cDIP when $B_{TX} = 6$ bits. This shows the requirement of some intelligence at the Tx end in order to obtain a high D_T. cDIP and AP2 [20] use the additional knowledge of X_0 and hence they are able to achieve relatively higher D_T compared to AP1 and CT. Here, note that AP2 use the knowledge of X_0 only when $X_0 < X_{TH}$. It fails to sufficiently exploit the channel when $X_0 \geq X_{TH}$. However, cDIP uses the knowledge of X_0 in both the scenarios, i.e., $X_0 < X_{TH}$ and $X_0 \geq X_{TH}$, which results in its consistently better performance than its nearest competitor AP2 in terms of higher D_T; the gain margin being approximately 40.18%.

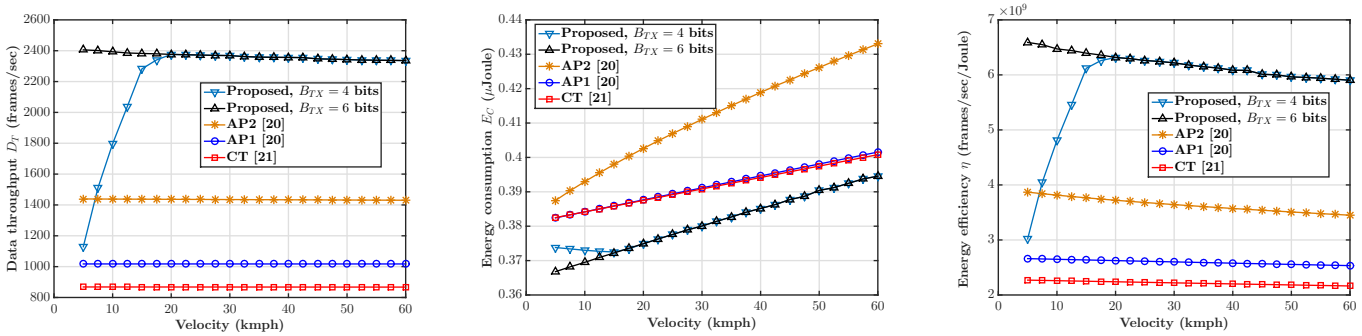

(a) (b) (c)

Fig. 6. Performance comparison: (a) Data throughput; (b) Energy consumption; (c) Energy efficiency. $X_{TH} = -3.9788$ dBm.

Further, the plots in Fig. 6(a) also demonstrate the role of extra overhead of cDIP that was discussed in Section V-C. At a lower node velocity, lower B_{TX} badly affects the performance of cDIP, resulting in very low D_T. But the situation improves with increasing node velocity.

2) Energy consumption E_C: For comparison of energy consumption E_C, values of I_t, I_r, and I_w are taken from Chipcon $CC1000$ data sheet [51]: $I_t = 17.5$ mA, $I_r = 19.7$ mA, and $I_w = 426$ mA, respectively, and $R = 1\ \Omega$.

An overall increasing trend of E_C with node velocity irrespective of the transmission scheme is observed in Fig. 6(b). Further, the energy consumption of AP1 and CT are almost identical. E_C of AP2 is higher compared to AP1 and CT, though by a small margin of approximately 7.25%. E_C corresponding to cDIP is the least compared to the existing protocols; which is approximately 8.89% less compared to AP2, when its corresponding D_T is approximately 40.18% more than that of AP2.

Moreover, E_C of cDIP with $B_{TX} = 4$ bits initially decreases, but at around $v = 17.5$ kmph it merges with the increasing trend of its counterpart with $B_{TX} = 6$ bits. The reason behind this counter-intuitive nature is that, when $B_{TX} = 4$ bits, the maximum possible transferred value of $\boldsymbol{T_{gb}}$ is 16 even though the actual value is considerably higher. The values of both $\boldsymbol{T_{gb}}$ and $\boldsymbol{T_{bg}}$ decrease with increasing v (as also observed from Fig. 3) leading to increase in E_C, as from (23) it can be seen that E_C is a function of both $\boldsymbol{T_{gb}}$ and $\boldsymbol{T_{bg}}$. Fig. 6(b) in a way also reinforces the observation made in Fig. 5, i.e., the performance of cDIP saturates at around $v = 18$ kmph with $B_{TX} = 4$ bits.

3) Energy efficiency η: Fig. 6(c) shows the variation of η against node velocity for all the schemes. The figure shows that both AP1 and CT offer η in the range of less than 3×10^9 frames/sec/Joule, which is approximately 59.63% lesser compared to cDIP. Even when compared to its nearest competitor AP2, there exists a consistent gap of approximately 41.29%. Combining this fact along with approximately 40.18% higher data throughput and approximately 9% lower energy consumption compared to its nearest competitor AP2, clearly establishes the advantage of the proposed cDIP.

VI. Conclusion

In this work an energy-efficient transmission protocol, called cDIP, has been proposed for link-layer communication. It intelligently estimates the subsequent waiting interval as well as the continuous transmission duration depending on the present channel state. cDIP gets rid of unnecessary probing of the channel, and is suitable for a range of IoT communications over short-range wireless links. It has been demonstrated through numerical results and extensive simulations that, irrespective of the underlying fading distribution, cDIP offers high data throughput and energy efficiency simultaneously, at the expense of negligibly-small additional overhead bits.

References

[1] "On the pulse of the networked society," Ericsson Mobility Report, Jun. 2017.

[2] G. Y. Li, Z. Xu, C. Xiong, C. Yang, S. Zhang, Y. Chen, and S. Xu, "Energy-efficient wireless communications: Tutorial, survey, and open issues," *IEEE Wireless Commun. Mag.*, vol. 18, no. 6, pp. 28–35, Dec. 2011.

[3] I. Chih-Lin, C. Rowell, S. Han, Z. Xu, G. Li, Z. Pan, "Toward green and soft: A 5G perspective," *IEEE Commun. Mag.*, vol. 52, no. 2, pp. 66–73, Feb. 2014.

[4] S. Bi, Y. Zeng, and R. Zhang, "Wireless powered communication networks: An overview," *IEEE Wireless Commun. Mag.*, vol. 23, no. 2, pp. 10–18, Apr. 2016.

[5] D. L. Lu and J. F. Chang, "Performance of ARQ protocols in nonindependent channel errors," *IEEE Trans. Commun.*, vol. 41, no. 5, pp. 721–730, May 1993.

[6] S. Li and Y. Zhou, "Performance analysis of SR-ARQ based on Geom/G/1/∞ queue over wireless link," *Appl. Math*, vol. 7, no. 5, pp. 1969–1976, 2013.

[7] J. Cloud, D. Leith, and M. Medard, "A coded generalization of selective repeat ARQ," in *Proc. IEEE INFOCOM*, Kowloon, Hong Kong, Apr. 2015, pp. 2155–2163.

[8] S. Chakraborty, M. Liinaharja, and P. Lindroos, "Analysis of adaptive GBN schemes in a Gilbert-Elliott channel and optimisation of system parameters," *Elsevier Comput. Netw.*, vol. 48, no. 4, pp. 683 – 695, 2005.

[9] K. Ausavapattanakun and A. Nosratinia, "Analysis of Go-Back-N ARQ in block fading channels," *IEEE Trans. Wireless Commun.*, vol. 6, no. 8, pp. 2793–2797, Aug. 2007.

[10] C. Pimentel and R. L. Siqueira, "Analysis of the Go-Back-N protocol on finite-state Markov Rician fading channels," *IEEE Trans. Veh. Technol.*, vol. 57, no. 4, pp. 2627–2632, July 2008.

[11] G. Benelli and A. Garzelli, "New modified stop-and-wait ARQ protocols for mobile communications," *Wirel. Pers. Commun.*, vol. 1, no. 2, pp. 117–126, 1994.

[12] S. W. S. De Vuyst and H. Bruneel, "Delay analysis of the stop-and-wait ARQ protocol over a correlated error channel," in *Proc. HETNETs*, Ukley, West Yorkshire, UK, July 2004.

[13] J. Li and Y. Q. Zhao, "Resequencing analysis of Stop-and-Wait ARQ for parallel multichannel communications," *IEEE/ACM Trans. Netw.*, vol. 17, no. 3, pp. 817–830, June 2009.

[14] Q. Liu, S. Zhou, and G. Giannakis, "Cross-layer combining of adaptive modulation and coding with truncated ARQ over wireless links," *IEEE Trans. Wireless Commun.*, vol. 3, no. 5, pp. 1746–1755, Sep. 2004.

[15] N. Wang and T. A. Gulliver, "Cross layer AMC scheduling for a cooperative wireless communication system over Nakagami-m fading channels," *IEEE Trans. Wireless Commun.*, vol. 11, no. 6, pp. 2330–2341, June 2012.

[16] J. Ramis and G. Femenias, "Cross-layer QoS-constrained optimization of adaptive multi-rate wireless systems using infrastructure-based cooperative ARQ," *IEEE Trans. Wireless Commun.*, vol. 12, no. 5, pp. 2424–2435, May 2013.

[17] K. J. Guth and T. T. Ha, "An adaptive stop-and-wait ARQ strategy for mobile data communications," in *Proc. IEEE VTC Spring*, Orlando, USA, May 1990.

[18] H. Minn, M. Zeng, and V. K. Bhargava, "On ARQ scheme with adaptive error control," *IEEE Trans. Veh. Technol.*, vol. 50, no. 6, pp. 1426–1436, Nov. 2001.

[19] M. Zorzi and R. R. Rao, "Error control and energy consumption in communications for nomadic computing," *IEEE Trans. Comput.*, vol. 46, no. 3, pp. 279–289, Mar. 1997.

[20] S. De, A. Sharma, R. Jantti, and D. Cavdar, "Channel adaptive stop-and-wait automatic repeat request protocols for short-range wireless links," *IET Commun.*, vol. 6, no. 14, pp. 2128–2137, Sep. 2012.

[21] H. Moon, "Channel-adaptive random access with discontinuous channel measurements," *IEEE J. Sel. Areas Commun.*, vol. 34, no. 5, pp. 1704–1712, May 2016.

[22] P. Mukherjee, D. Mishra, and S. De, "Exploiting temporal correlation in wireless channel for energy-efficient communication," *IEEE Trans. Green Comm. and Networking*, vol. 1, no. 4, pp. 381–394, Dec. 2017.

[23] S. Agarwal and S. De, "Impact of channel switching in energy constrained cognitive radio networks," *IEEE Commun. Lett.*, vol. 19, no. 6, pp. 977–980, June 2015.

[24] ——, "eDSA: Energy-efficient dynamic spectrum access protocols for cognitive radio networks," *IEEE Trans. Mobile Comput.*, vol. 15, no. 12, pp. 3057–3071, Dec. 2016.

[25] Z. Rosberg and N. Shacham, "Resequencing delay and buffer occupancy under the selective-repeat ARQ," *IEEE Trans. Inf. Theory*, vol. 35, no. 1, pp. 166–173, Jan. 1989.

[26] S. Tripathi and S. De, "An efficient data characterization and reduction scheme for smart metering infrastructure," *IEEE Trans. Ind. Informat.*, Jan. 2018, (In Press, DOI: 10.1109/TII.2018.2799855).

[27] *IEEE Standard for Synchrophasor Measurements for Power Systems*, IEEE Std C37.118.1-2011 ed., 2011.

[28] A. Unterweger and D. Engel, "Resumable load data compression in smart grids," *IEEE Trans. Smart Grid*, vol. 6, no. 2, pp. 919–929, Mar. 2015.

[29] S. Tripathi and S. De, "Dynamic prediction of powerline frequency for wide area monitoring and control," *IEEE Trans. Ind. Informat.*, Dec. 2017, (In Press, DOI: 10.1109/TII.2017.2777148).

[30] W. Yao, L. Zhan, Y. Liu, M. J. Till, J. Zhao, L. Wu, Z. Teng, and Y. Liu, "A novel method for phasor measurement unit sampling time error compensation," *IEEE Trans. Smart Grid*, vol. 9, no. 2, pp. 1063–1072, Mar. 2018.

[31] C. Campolo, A. Molinaro, A. Vinel, and Y. Zhang, "Modeling and enhancing infotainment service access in vehicular networks with dual-radio devices," *Elsevier Veh. Commun.*, vol. 6, pp. 7 – 16, 2016.

[32] E. Belyaev, P. Molchanov, A. Vinel, and Y. Koucheryavy, "The use of automotive radars in video-based overtaking assistance applications," *IEEE Trans. Intell. Transp. Syst.*, vol. 14, no. 3, pp. 1035–1042, Sep. 2013.

[33] S. De and R. Singhal, "Toward uninterrupted operation of wireless sensor networks," *IEEE Computer Mag.*, vol. 45, no. 9, pp. 24–30, Sep. 2012.

[34] O. Briante, C. Campolo, A. Iera, A. Molinaro, S. Y. Paratore, and G. Ruggeri, "Supporting augmented floating car data through smartphone-based crowd-sensing," *Elsevier Veh. Commun.*, vol. 1, no. 4, pp. 181 – 196, 2014.

[35] N. M. Balasubramanya, L. Lampe, G. Vos, and S. Bennett, "DRX with quick sleeping: A novel mechanism for energy-efficient IoT using LTE/LTE-A," *IEEE Internet Things J.*, vol. 3, no. 3, pp. 398–407, June 2016.

[36] M. Siekkinen, E. Masala, and J. K. Nurminen, "Optimized upload strategies for live scalable video transmission from mobile devices," *IEEE Trans. Mob. Comput.*, vol. 16, no. 4, pp. 1059–1072, Apr. 2017.

[37] C. Tepedelenlioglu, A. Abdi, G. B. Giannakis, and M. Kaveh, "Estimation of doppler spread and signal strength in mobile communications with applications to handoff and adaptive transmission," *Wireless Commun. Mob. Comput.*, vol. 1, no. 2, pp. 221–242, 2001.

[38] M. Zorzi, R. R. Rao, and L. B. Milstein, "ARQ error control for fading mobile radio channels," *IEEE Trans. Veh. Technol.*, vol. 46, no. 2, pp. 445–455, May 1997.

[39] A. Borhani and M. Ptzold, "Correlation and spectral properties of vehicle-to-vehicle channels in the presence of moving scatterers," *IEEE Trans. Veh. Technol.*, vol. 62, no. 9, pp. 4228–4239, Nov 2013.

[40] M. K. Simon and M. Alouini, "A unified approach to the performance analysis of digital communication over generalized fading channels," *Proc. IEEE*, vol. 86, no. 9, pp. 1860–1877, Sep. 1998.

[41] S. L. Cotton, "Second-order statistics of $\kappa - \mu$ shadowed fading channels," *IEEE Trans. Veh. Technol.*, vol. 65, no. 10, pp. 8715–8720, Oct. 2016.

[42] W. C. Horrace, "Some results on the multivariate truncated normal distribution," *Journal of Multivariate Analysis*, vol. 94, no. 1, pp. 209–221, 2005.

[43] A. Genz, "Numerical computation of multivariate normal probabilities," *Journal of computational and graphical statistics*, vol. 1, no. 2, pp. 141–149, 1992.

[44] A. Mattuck, *Introduction to Analysis*. Prentice Hall, 1999.

[45] W. Rudin, *Principles of Mathematical Analysis*. McGraw-Hill Publishing Co., 1976.

[46] A. D. Belegundu and T. R. Chandrupatla, *Optimization Concepts and Applications in Engineering*. Cambridge University Press, 2011.

[47] J. F. Bonnans, J. C. Gilbert, C. Lemaréchal, and C. A. Sagastizábal, *Numerical Optimization: Theoretical and Practical Aspects*. Springer-Verlag, 2006.

[48] F. Meshkati, H. V. Poor, and S. C. Schwartz, "Energy-efficient resource allocation in wireless networks," *IEEE Signal Process. Mag.*, vol. 24, no. 3, pp. 58–68, May 2007.

[49] A. Goldsmith, *Wireless Communications*. Cambridge University Press, 2005.

[50] T. Rappaport, *Wireless Communications: Principles and Practice*, 2nd ed. Upper Saddle River, NJ, USA: Prentice Hall PTR, 2001.

[51] *Chipcon CC1000 Datasheet*, Texas Instruments, [Online]. Available: http://www.ti.com/lit/ds/symlink/cc1000.pdf.

Priyadarshi Mukherjee received the B. Tech. degree in Electronics and Communication Engineering from Kalyani Government Engineering College, West Bengal University of Technology, Kolkata, India, in 2012 and the M.E. degree from Department of Electronics and Telecommunication Engineering, Indian Institute of Engineering Science and Technology (IIEST), Shibpur, in 2014. He is currently pursuing the Ph.D. degree in Department of Electrical Engineering, Indian Institute of Technology Delhi, India. His research interests include performance modeling and analysis of wireless channels, green communications, computer networks, cognitive radio networks, and MIMO systems.

Swades De (S'02-M'04-SM'14) received his B.Tech. degree in Radiophysics and Electronics from the University of Calcutta in 1993, the M.Tech. degree in Optoelectronics and Optical communication from IIT Delhi in 1998, and the Ph.D. degree in Electrical Engineering from the State University of New York at Buffalo in 2004.

He is currently a Professor with the Department of Electrical Engineering, IIT Delhi. Before moving to IIT Delhi in 2007, he was a Tenure-Track Assistant Professor with the Department of ECE, New Jersey Institute of Technology, Newark, NJ, USA, from 20042007. He worked as an ERCIM Post-doctoral Researcher at ISTI-CNR, Pisa, Italy (2004), and has nearly five years of industry experience in India on telecom hardware and software development, from 19931997, 1999. His research interests are broadly in communication networks, with emphasis on performance modeling and analysis. Current directions include energy harvesting sensor networks, broadband wireless access and routing, cognitive/white-space access networks, smart grid networks, and IoT communications. Dr. De currently serves as a Senior Editor of IEEE COMMUNICATIONS LETTERS, and an Associate Editor of IEEE TRANSACTIONS ON VEHICULAR TECHNOLOGY, IEEE WIRELESS COMMUNICATIONS LETTERS, Springer Photonic Network Communications, and the IETE Technical Review Journal.